

# Modification of Inorganic Supports with Nickel Acetylacetonate: The Effect of Their Surface Properties

I. A. Ledenev<sup>a</sup>, R. V. Prikhod’ko<sup>a</sup>, I. V. Stolyarova, E. J. M. Hensen<sup>b</sup>,  
J. A. R. van Veen<sup>c</sup>, M. V. Sychev<sup>a</sup>, and V. V. Goncharuk<sup>a</sup>

<sup>a</sup> Dumanskii Institute of Colloid and Water Chemistry, National Academy of Sciences of Ukraine, Kiev, Ukraine

<sup>b</sup> Technical University of Eindhoven, the Netherlands

<sup>c</sup> Shell International Chemicals, Amsterdam, the Netherlands

Received November 12, 2004

**Abstract**—The mesostructured silica SBA-15,  $\gamma$ -Al<sub>2</sub>O<sub>3</sub>, and amorphous silica–alumina are modified with Ni(acac)<sub>2</sub> in the liquid and gas phases. This process depends crucially on the nature of active sites on the support surface. In the modification of materials containing weakly acidic or weakly basic hydroxyl groups, it is necessary to use low-polarity solvents. The dominant Ni(acac)<sub>2</sub> chemisorption sites on amorphous silica–alumina are the acid hydroxyls of  $\equiv$ Si–OH–Al= bridges. The covalent bonding resulting from the replacement of the acetylacetonate ligand favors the fixation of the adsorbed complex on the support surface. The coordinatively unsaturated sites formed by Al<sup>3+</sup> ions play an insignificant role in Ni(acac)<sub>2</sub> chemisorption. The degree of dispersion of the oxide phase in the resulting catalysts depends strongly on the strength of the interaction between the modifier molecules and the active sites of the support. This is not the case with the aluminum acetylacetonate complexes that form upon the modification of the Al-containing supports. Gas-phase modification affords finer NiO particles than liquid-phase modification.

**DOI:** 10.1134/S0023158406030189

Transition metal oxides (including nickel oxide) fixed on inorganic supports such as  $\gamma$ -Al<sub>2</sub>O<sub>3</sub>, SiO<sub>2</sub>, TiO<sub>2</sub>, and aluminosilicates are efficient catalysts for a wide variety of commercial processes, including the hydrotreating of petroleum, the selective reduction of nitrogen oxides, the low-temperature oxidation of carbon monoxide, and partial methane oxidation [1–4]. The high thermal stability and the large specific surface area of these supports and specific oxide–support interactions enhance the stability and activity of the catalysts [5]. The catalytic properties of such catalysts depend strongly on the degree of dispersion of the active phase and on the uniformity of the distribution of this phase on the surface. Therefore, a search for new ways of controlling these parameters is an important line in the advancement of preparative methods for this class of catalysts.

One of the most promising methods of catalyst preparation is atomic layer deposition [6], which enables one to form finely dispersed, uniformly distributed active phases. The essence of this method is that a metal acetylacetonate complex is chemisorbed onto the support surface and is then thermally decomposed in an oxygen-containing atmosphere. Such modification can be carried out either in an organic solvent or via metal acetylacetonate sublimation in a flowing inert gas [7]. The interaction between the complex and the support surface depends strongly on the molecular geometry and coordination state of the complex [7, 8]. For exam-

ple, the pyramidal complex VO(acac)<sub>2</sub> and the planar complex Cu(acac)<sub>2</sub> are chemisorbed more readily than the sterically hindered, coordinatively saturated complexes (e.g., Cr(acac)<sub>3</sub>) [7].

According to current views [5, 7, 8], the acetylacetonate complexes are chemisorbed through the formation of a hydrogen bond between an acetylacetonate ligand and a surface hydroxyl group or through the displacement of a ligand and the formation of a covalent bond between the metal atom and a surface oxygen atom [7]. The heterogeneity of the active sites of the support can complicate this process and eventually affect the degree of dispersion of the metal oxide phase. This is particularly true for alumina and aluminosilicates, since their surface has acid, neutral, and base hydroxyl groups and coordinatively unsaturated sites formed by Al<sup>3+</sup> cations [5]. This point has not been adequately investigated. Therefore, the purpose of this study is to see how the modification of alumina, aluminosilicates, and mesostructured silica with nickel acetylacetonate depends on the nature of the active sites.

## EXPERIMENTAL

### *Preparation of Supports*

Mesostructured silica (SBA-15) was prepared by a procedure similar to the procedure used by Yamada et al. [9]. The triblock copolymer EO<sub>20</sub>PO<sub>70</sub>EO<sub>20</sub>

(BASF Pluronic P123; EO = ethylene oxide, and PO = propylene oxide) was the structure-forming agent, and tetraethyl orthosilicate ( $\text{Si}(\text{OC}_2\text{H}_5)_4$ , TEOS) was the source of silicon. The molar composition of the reaction mixture was TEOS : P123 : HCl :  $\text{H}_2\text{O} = 1 : 0.017 : 5.7 : 193$ .  $\text{EO}_{20}\text{PO}_{70}\text{EO}_{20}$  was dissolved in hydrochloric acid, and TEOS was added to the solution under vigorous stirring. The mixture was held at 353 K for 24 h without stirring. The resulting precursor of SBA-15 was filtered out, washed thrice with distilled water and twice with ethanol, and dried at 373 K in flowing air for 18 h. The copolymer was removed by calcining the precursor in flowing air for 5 h while raising the temperature to 832 K at a rate of 1 K/min.

In the synthesis of amorphous silica–alumina (ASA) with  $\text{Si}^{4+} : \text{Al}^{3+} = 6.0$ ,  $\text{AlCl}_3 \cdot 6\text{H}_2\text{O}$  (10.75 g) and  $\text{Na}_2\text{SiO}_3 \cdot 9\text{H}_2\text{O}$  (60 g) were dissolved in water (400 cm<sup>3</sup>) and glacial  $\text{CH}_3\text{COOH}$  (35 cm<sup>3</sup>) was added. Thereafter,  $\text{NH}_4\text{OH}$  (25%) was added in drops to the stirred solution so as to maintain pH 7.1. The resulting gel was stirred for 1 h, filtered, washed with a hot (363 K) 0.25 M  $\text{CH}_3\text{COONH}_4$  solution five times, dried at 343 K for 24 h, and calcined at 953 K for 7 h.

Another support examined was commercial  $\gamma\text{-Al}_2\text{O}_3$  (CR 300, Ketjen).

### Modification of Supports

Before liquid-phase modification, the adsorbed water was removed from the supports by pumping them at 523 K for 2 h. Thereafter, the reactor was cooled to room temperature and filled with dry argon, nickel acetylacetone dissolved in toluene (while heating) or in dimethylformamide (DMF) was added, and the mixture was stirred for 3 h. The solid phase was separated by centrifugation, washed with fresh solvent, and dried in *vacuo*. The concentration of the sorbed complex was determined photometrically on a Specord UV-VIS M 40 spectrophotometer (Carl Zeiss Jena).

For gas-phase modification, 0.5 g of the support was placed into a glass flow reactor with a porous glass bottom and was heat-treated at 523 K for 2 h in flowing dry  $\text{N}_2$  (25 cm<sup>3</sup>/min). This enabled us to remove the physically adsorbed water. Next, the reactor was cooled to 493 K and the vessel containing the modifier was moved from the cold zone to the hot zone of the reactor. The instant condensed acetylacetone appeared at the reactor outlet was considered to be the end point of chemisorption. After that, the modifier container was returned to its original place. The unreacted acetylacetone was removed by purging the reactor with nitrogen at 493 K for 3 h. Thereafter, the reactor was cooled to room temperature and the resulting material was transferred to an airtight vessel.

In order to obtain supported catalysts, the specimens modified by both methods were calcined in flowing air, raising the temperature to 723 K at a rate of 10 K/min.

### Experimental Methods

X-ray diffraction patterns from SBA-15 and its precursor were recorded on a Rigaku RINT-2000 diffractometer (Ni-filtered  $\text{CuK}_\alpha$  radiation) in a Bragg angle range of  $(2\theta) 1.5^\circ\text{--}10^\circ$  with a scan step of 1 deg/min.

Nitrogen adsorption and desorption isotherms (at 77 K) were obtained on a Micrometrics ASAP 2010 adsorption unit for samples preliminarily pumped at 473 K for 5 h. Pore-size distribution was determined by processing the desorption isotherms using the Barrett–Joyner–Halenda method [10].

IR spectra were recorded on a Nicolet Avatar 360 FT-IR spectrophotometer. The samples to be examined were pressed into pellets with thoroughly dried KBr (1 : 60).

High-resolution magic-angle-spinning (MAS) and two-dimensional multiquantum magic-angle-spinning (MQ MAS)  $^{27}\text{Al}$  NMR spectra were recorded on a Bruker Avance 500 spectrometer operating at a magnetic resonance frequency of 130 MHz and a spinning frequency of 28 kHz. The base line artifacts in the one-dimensional NMR spectra were suppressed using a two-pulse spin echo sequence. The radio-frequency field was 50 kHz. The duration of the first and second pulses was 2 and 4  $\mu\text{s}$ , respectively. The spin echo generation delay was 10  $\mu\text{s}$ . Each spectrum was made up of 256 to 1024 accumulated scans. The relaxation delay was 1 s. The chemical shift of  $^{27}\text{Al}$  lines was determined relative to an external saturated solution of  $\text{Al}(\text{NO}_3)_3$ . The isotropic chemical shift in the second dimension of MQ MAS spectra was determined by the shearing procedure. The NMR spectra were processed using the Xwin-NMR program (Bruker).

Thermogravimetric and differential thermal analyses (DTG–DTA) were carried out on an STA-1500H thermoanalytical system in flowing air (50 cm<sup>3</sup>/min) at a heating rate of 10 K/min.

The nickel content of the catalysts prepared by the calcination of modified supports was determined by atomic absorption spectroscopy on a Perkin-Elmer PE 3030 spectrophotometer.

The proton-donor acid sites on the support surface were quantified by the temperature-programmed decomposition of adsorbed isopropylamine [11, 12]. Samples were heat-treated in flowing helium (100 cm<sup>3</sup>/min) for 1 h at 723 K (heating rate 2 K/min) and were then cooled to 323 K, and isopropylamine was adsorbed from its saturated vapor. Adsorption was considered to be complete once excess amine was detected mass-spectrometrically (Balzers quadrupole MS mass spectrometer). The physically adsorbed isopropylamine was removed by blowing the sample with helium at 323 K for 16 h. For temperature-programmed decomposition, the sample was heated to 773 K at a rate of 5 K/min. The surface concentration of acid sites was determined mass-spectrometrically in terms of the propylene released, assuming that one proton-donor site chemisorbs one amine molecule [11, 12].

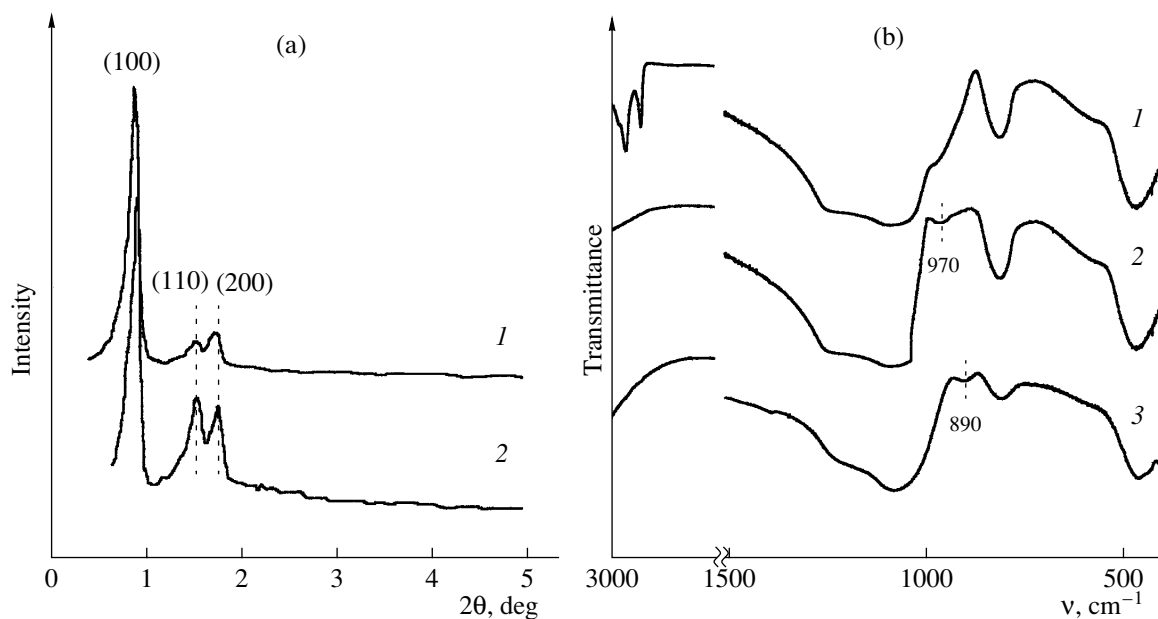


Fig. 1. (a) X-ray diffraction patterns and (b) IR spectra of (1) the SBA-15 precursor, (2) calcined SBA-15, and (3) ASA.

The  $\text{H}_2$  TPR profiles for supported catalysts were obtained using a flow reactor connected to a thermal-conductivity detector. The sample was reduced with a hydrogen–argon mixture (66%  $\text{H}_2$ ) flowing at a rate of 20  $\text{cm}^3/\text{min}$ . The temperature range was 298–1073 K, and the heating rate was 5 K/min.

The degree of dispersion of the  $\text{NiO}$  phase was determined by  $\text{H}_2$  chemisorption in an adsorption unit fitted with an MKS Baratron pressure sensor. Prior to measurements, the sample was heated in the measurement cell at 453 K in a nitrogen atmosphere. The  $\text{N}_2$  flow rate was 40  $\text{cm}^3/\text{min}$  and the heating rate was 5 K/min. Thereafter, the sample was reduced with a nitrogen–hydrogen mixture (50%  $\text{H}_2$ ) at 673 K for 1.5 h. Next, the sample was cooled to 473 K while pumping and  $\text{H}_2$  was adsorbed at this temperature for 0.7 h. Thereafter, the cell was cooled to 295 K and a hydrogen desorption isotherm was measured at partial pressures of 133–1.33 kPa. The  $\text{H}_2$  : Ni ratio, which is a measure of the degree of dispersion of the metal-containing phase [6, 13], was found by extrapolating the isotherm to zero  $\text{H}_2$  pressure.

## RESULTS AND DISCUSSION

### *Characterization of Supports*

The X-ray diffraction pattern from the precursor of SBA-15 (Fig. 1a) shows the basal reflections (100), (110), and (200) at  $2\theta = 1^\circ$ – $4^\circ$ . These reflections are characteristic of this mesostructured silica [9, 14], which crystallizes in a hexagonal system (space group  $P6mm$ ) [14]. The IR spectrum of this precursor (Fig. 1b) exhibits absorption bands at 1240, 1070, 970, 800, 575, and 455  $\text{cm}^{-1}$ , which are due to the stretching

vibrations of the structural fragments  $\text{Si}=\text{O}=\text{Si}$ ,  $\text{Si}=\text{O}$ ,  $\text{Si}=\text{OH}$ , and  $\text{Si}=\text{O}$  [15], and absorption bands between 2800 and 3000  $\text{cm}^{-1}$ , which are due to the stretching vibrations of the C–H bonds in the structure-forming agent. After the material was calcined in flowing air, the latter bands were no longer observed, indicating that all of the organic phase was removed. The other bands appeared to be slightly shifted, but their intensities were unchanged. Calcination did not cause any significant weakening or broadening of the diffraction peaks (Fig. 1a). Therefore, the removal of the structure-forming agent did not cause any structural disorder in SBA-15.

The  $\text{N}_2$  adsorption isotherm for calcined SBA-15 (Fig. 2a) can be assigned to type IV according to the IUPAC classification [16]. Therefore, the texture of SBA-15 is mesoporous. However, part of the porous structure of this material is formed by micropores, as is evident from the  $t$ -plot (Fig. 2b) derived from the adsorption isotherm. Micropores can be situated in the walls of tubular channels [9], and their contribution to the total specific surface area can be ~30% (Table 1). Nevertheless, most of the porous structure of this material is due to uniformly sized pores of diameter ~7.5 nm (Fig. 2c). These results are in agreement with the literature [9, 14] and suggest that the material synthesized is the well-ordered mesostructured silica SBA-15.  $\gamma\text{-Al}_2\text{O}_3$  used in this study also has a mesoporous structure (Table 1).

The amorphous silica–alumina synthesized is also mesoporous, and its nitrogen adsorption isotherm is distorted type IV (Fig. 2a). Most of its porous structure is formed by 3.4- to 4.2-nm pores (Fig. 2c). The IR spectrum of ASA (Fig. 1b) shows absorption bands at

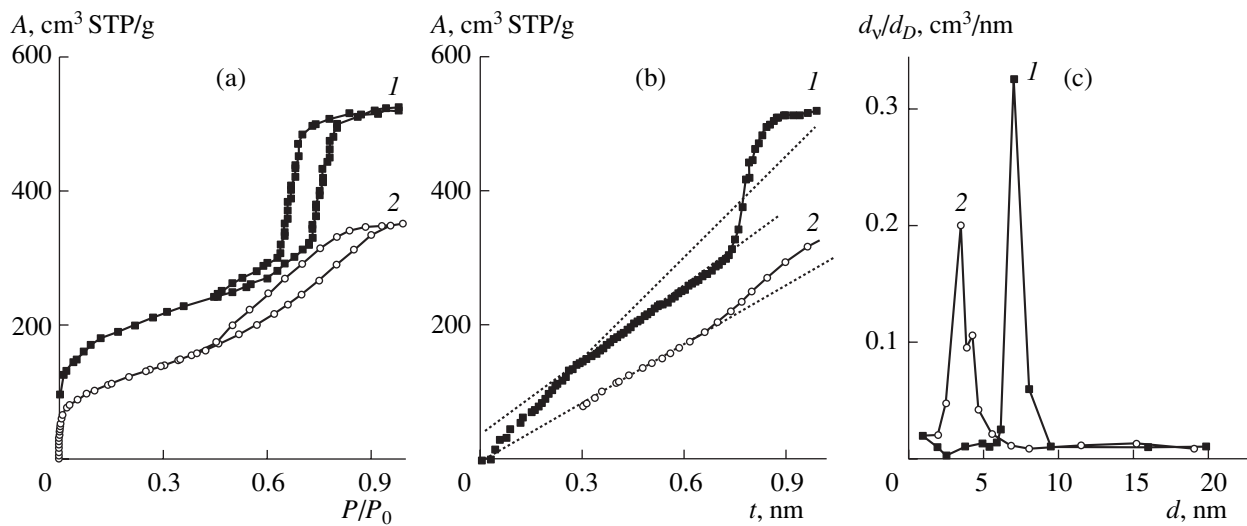


Fig. 2. (a) Nitrogen adsorption isotherms, (b)  $t$ -plots, and (c) pore-size distribution for (1) SBA-15 and (2) ASA.

1215, 1070, 797, and 452  $\text{cm}^{-1}$ , which are due to vibrations of the Si–O–Si, Si–O, Si–OH, and Si–O bonds [17], and a band at 890  $\text{cm}^{-1}$ , which indicates the presence of  $\equiv\text{Si}=\text{O}=\text{Al}=\equiv$  fragments.

The  $^{27}\text{Al}$  NMR spectrum of  $\gamma\text{-Al}_2\text{O}_3$  (which was used as the reference sample) contains signals from tetrahedrally and octahedrally coordinated  $\text{Al}^{3+}$  [18] with chemical shifts ( $\delta$ ) of about 70.0 and 5.0 ppm, respectively (Fig. 3). The spectrum of ASA shows an extra resonance at  $\delta = 30$  ppm, which is assignable to pentacoordinated aluminum [19]. This assignment was verified by MQ MAS NMR spectroscopy [20]. This technique allows the spectral resolution for quadrupole nuclei with a half-integer spin in the solid state to be significantly enhanced by suppressing the secondary quadrupole line broadening in the second dimension of the two-dimensional spectrum. Furthermore, the distribution of spectral lines over two dimensions makes the interpretation of the spectrum more reliable. The MQ MAS spectrum of ASA (Fig. 3b) shows a well-defined signal centered at  $\delta = 31$  ppm, which is missing in the spectrum of  $\gamma\text{-Al}_2\text{O}_3$ . Therefore, this line is not an artifact and should not be viewed as a spinning satellite or a result of a distortion of the quadrupole line. It is indeed due to pentacoordinated  $\text{Al}^{3+}$  in ASA. The signal from tetracoordinated  $\text{Al}^{3+}$  in the NMR spectrum of

ASA is shifted downfield relative to the same line in the spectrum of  $\gamma\text{-Al}_2\text{O}_3$  (Fig. 3). By analogy with zeolites, this can be explained by the effect of the  $\text{Si}^{4+}$  ions in the  $\equiv\text{Si}=\text{O}=\text{Al}=\equiv$  fragments. The hydroxyl bridge in these fragments is a proton donor or, in other terms, is a Brønsted acid site. The amount of these sites was estimated at 0.32 mmol/g by temperature-programmed isopropylamine decomposition.

#### Liquid-Phase Modification

In the liquid-phase modification of a support, the solvent should not interact with the acetylacetone complex or the active sites of the surface. Therefore, it is of crucial importance to choose an appropriate solvent [7, 8]. The chemisorption of a metal acetylacetone can also be hampered by a solvation effect [7, 8, 21]. Therefore, water, which is widely employed in the impregnation methods of catalyst preparation, is inappropriate in this case.

In the modification of SBA-15 and  $\gamma\text{-Al}_2\text{O}_3$ , the amount of adsorbed  $\text{Ni}(\text{acac})_2$  depends strongly on the polarity of the solvent. In the case of ASA, this dependence is not observed (Fig. 4). The micropores and mesopores in the silica structure favor  $\text{Ni}(\text{acac})_2$  adsorption in DMF, a polar solvent with  $\mu = 1.67 \text{ D}$ . As

Table 1. Pore structure parameters of the supports

Support	$S_{\text{sp}}$ , $\text{m}^2/\text{g}$	$S_{\text{meso}}$ , $\text{m}^2/\text{g}$	$S_{\text{micro}}$ , $\text{m}^2/\text{g}$	$V_{\text{lim}}$ , $\text{cm}^3/\text{g}$
SBA-15	770	550	220	0.81
$\text{Al}_2\text{O}_3$	190	180	10	0.66
ASA	400	400	—	0.54

Note:  $S_{\text{sp}}$  is the specific surface area determined by the BET method,  $S_{\text{meso}}$  and  $S_{\text{micro}}$  are the specific surface areas of the mesopores and micropores determined from the  $t$ -plot, and  $V_{\text{lim}}$  is the limiting sorption volume of the pores.

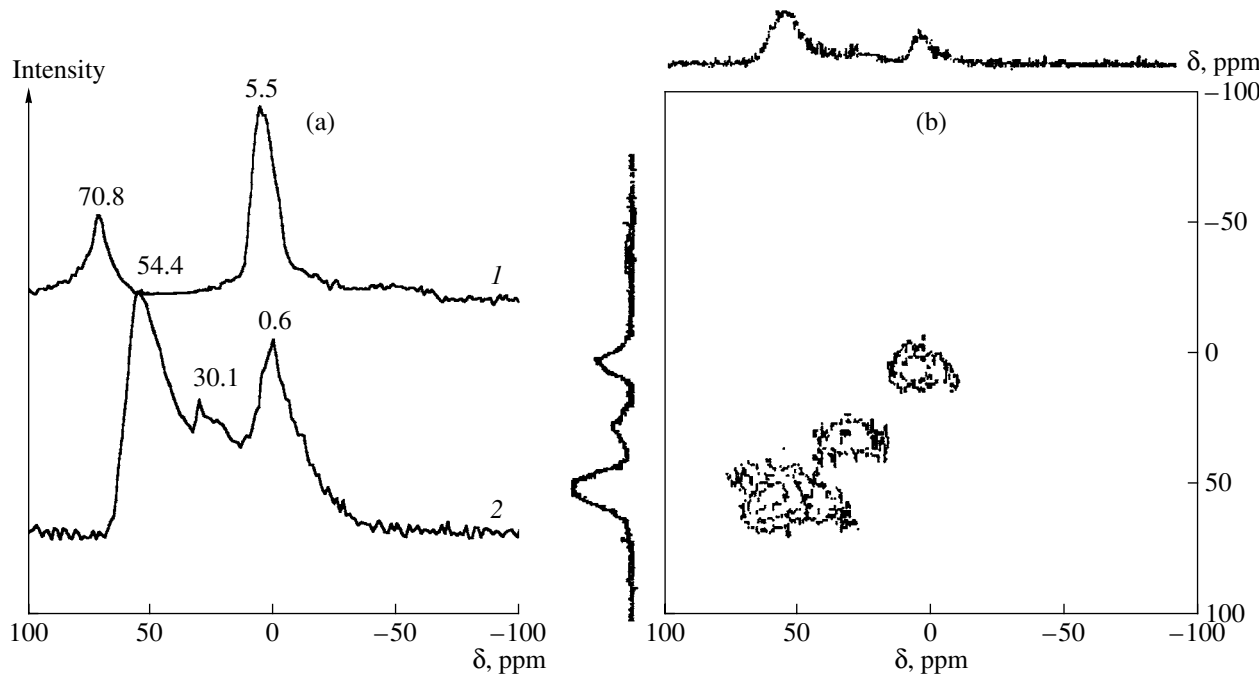


Fig. 3. (a) High-resolution and (b) multiquantum  $^{27}\text{Al}$  NMR spectra of (1)  $\gamma\text{-Al}_2\text{O}_3$  and (2) ASA.

is clear from Fig. 4, the mesostructured silica SBA-15 adsorbs nearly twice as much  $\text{Ni}(\text{acac})_2$  as nonporous  $\text{SiO}_2$  (Aerosil A-260, which is the reference sample). When toluene (a low-polarity liquid with  $\mu = 0.39$  D) is used as the solvent, the porous structure of the support is less significant and both materials show similar sorption capacities.

The effect of the solvent on the chemisorption of  $\text{Ni}(\text{acac})_2$  can be explained as follows. The polar solvent DMF is capable of neutralizing the weakly acidic and basic hydroxyl groups of silica and  $\gamma\text{-Al}_2\text{O}_3$ , thereby preventing their interaction with  $\text{Ni}(\text{acac})_2$  molecules. This view is supported by the low sorption capacity of nonporous  $\text{SiO}_2$ , whose active sites are most readily accessible to the solvent. Since these sites are neutralized on the silica and  $\gamma\text{-Al}_2\text{O}_3$  surfaces, the complex adsorbed on these materials is not bonded to the surface and is readily removed by washing (Fig. 4).

The absence of an adverse effect of DMF on ASA is due to the fact that,  $\text{Ni}(\text{acac})_2$ , which is an acid-sensitive compound [8], reacts mainly with the protons of  $\equiv\text{Si}-\text{OH}-\text{Al}=\text{}$  hydroxyl bridges. It was assumed that, because these sites are strongly acidic, DMF cannot neutralize them. This assumption was verified using ASA pretreated with 2,6-dimethylpyridine (2,6-DMP). Because of the steric effect of the two methyl groups, this base interacts primarily with proton-donor acid sites [22]. The poisoning of these sites was expected to markedly diminish the capacity of ASA for  $\text{Ni}(\text{acac})_2$  sorption. It was found that ASA treated with 2,6-DMP adsorbs  $\sim 75\%$  less  $\text{Ni}(\text{acac})_2$  than original ASA. This finding proves that the  $\equiv\text{Si}-\text{OH}-\text{Al}=\text{}$  hydroxyl bridges

of ASA are main  $\text{Ni}(\text{acac})_2$  chemisorption sites. The formation of a covalent bond through the replacement of an acetylacetone ligand with a proton binds the adsorbed complex to the ASA surface and prevents the removal of the complex as DMF is washed off (Fig. 4).

Toluene, which is a low-polarity solvent, does not block the active sites of the supports, and all of them remain accessible to  $\text{Ni}(\text{acac})_2$  molecules. This provides a plausible explanation for the fact that the  $\text{Ni}(\text{acac})_2$  sorption capacity of silica and  $\gamma\text{-Al}_2\text{O}_3$  is much higher in toluene than in DMF (Fig. 4). As was expected, the surface concentration of nickel atoms depends on the specific surface area of the support (Fig. 4).

This interpretation of the experimental data does not take into account that coordinatively unsaturated sites formed by  $\text{Al}^{3+}$  ions can be directly involved in  $\text{Ni}(\text{acac})_2$  chemisorption. As is demonstrated above, the neutralization of the acid hydroxyl groups of ASA does not completely suppress the adsorption of the complex on this material. The role of the coordinatively unsaturated sites was studied using  $\gamma\text{-Al}_2\text{O}_3$  and ASA pretreated with acetylacetone. The formation of  $\equiv\text{Si}-\text{OH}-\text{Al}=\text{}$  compounds on the surface selectively blocks these sites [5, 8]. If these sites were involved in  $\text{Ni}(\text{acac})_2$  chemisorption, this blocking would markedly reduce the sorption capacity of the support. In fact, acetylacetone treatment decreased the adsorption of the complex on the  $\gamma\text{-Al}_2\text{O}_3$  surface only by 0.04 mmol/g. Therefore, only a small proportion of the coordinatively unsaturated sites of alumina interacts with  $\text{Ni}(\text{acac})_2$ . A similar situation is observed with ASA, although the pentaco-

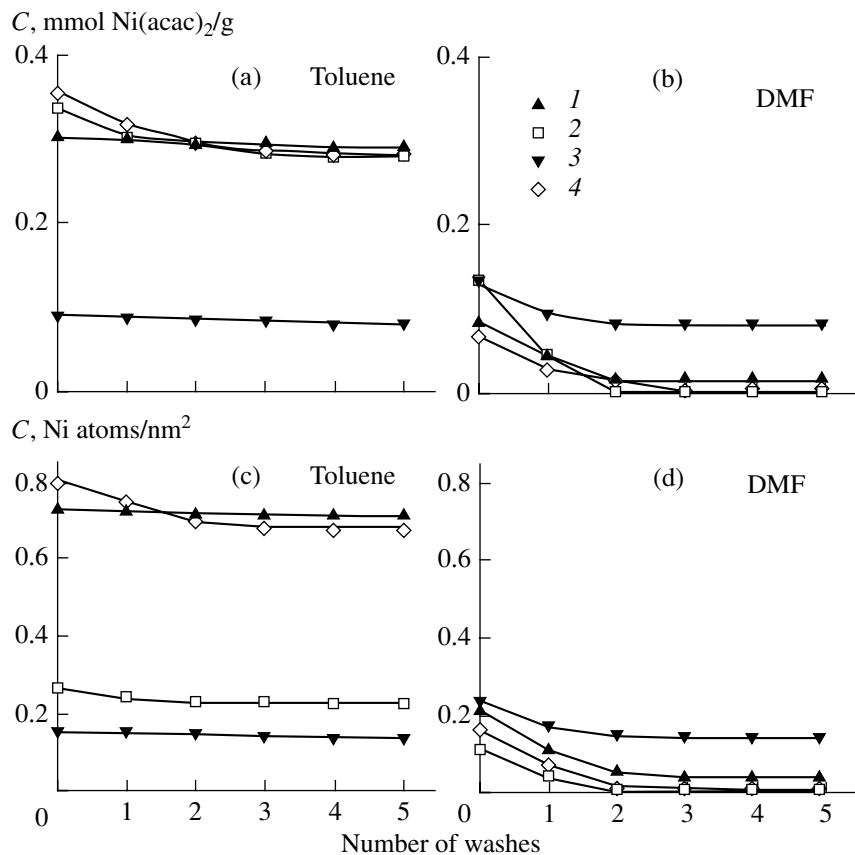


**Fig. 4.** Concentration of (a, b) adsorbed Ni(acac)<sub>2</sub> and (c, d) Ni<sup>2+</sup> ions versus the number of washes for (1)  $\gamma$ -Al<sub>2</sub>O<sub>3</sub>, (2) SBA-15, (3) ASA, and (4) nonporous SiO<sub>2</sub>. The washing liquid is (a, c) toluene and (b, d) DMF.

ordinated Al<sup>3+</sup> ions, with a highly unsaturated coordination sphere, were expected to favor localized Ni(acac)<sub>2</sub> adsorption. Thus, the coordinatively unsaturated sites formed by Al<sup>3+</sup> play only a negligible role in Ni(acac)<sub>2</sub> adsorption on the Al-containing supports.

Nickel acetylacetone can react with both acid and base sites [8]. Therefore, the acid hydroxyl bridges and base hydroxyl groups of ASA bonded to Al<sup>3+</sup> ions must be involved in the chemisorption of the complex. Since the blocking effect of DMF is much stronger for ASA than for  $\gamma$ -Al<sub>2</sub>O<sub>3</sub>, it is likely that the Al-OH groups of the former are more basic. Presumably, these sites are formed by pentacoordinated Al<sup>3+</sup> ions.

Calcined  $\gamma$ -Al<sub>2</sub>O<sub>3</sub> contains ~2.2 mmol/g of base hydroxyl groups [5]. However, it adsorbs only 0.3 mmol/g of Ni(acac)<sub>2</sub> in toluene (Fig. 4). Therefore, only part (~14%) of these groups can react with the complex. It is interesting that the same result was obtained in the modification of alumina with vanadium acetylacetone [5]. Since alumina and SBA-15 chemisorb nearly equal amounts of Ni(acac)<sub>2</sub> (Fig. 4), it is evident that equal numbers of hydroxyl groups in these supports react with the complex. The active sites of the ASA surface—bridging hydroxyls and base OH

groups—are more reactive: ~25% of them participate in Ni(acac)<sub>2</sub> chemisorption.

The thermal decomposition of the acetylacetones on the surface of the modified materials proceeds in several steps (Fig. 5). For all of these materials, the greatest weight loss is observed between 473 and 623 K and is primarily due to the oxidative decomposition of acetylacetone [5]. For SBA-15 and  $\gamma$ -Al<sub>2</sub>O<sub>3</sub>, some weight loss is also observed at 423–433 K. By analogy with VO(acac)<sub>2</sub> [5], this effect can be ascribed to the transformation of hydrogen-bonded Ni(acac)<sub>2</sub> into covalently bonded Ni(acac)<sub>2</sub>. Therefore, some of the complex reacts with surface hydroxyl groups of the supports to form hydrogen bonds. In the case of  $\gamma$ -Al<sub>2</sub>O<sub>3</sub>, the weight loss at 423–433 K is followed by weight losses at 548 and 598–600 K (Fig. 5). According to the literature [5, 23], these temperatures are, respectively, the points at which aluminum acetylacetone is converted to aluminum acetate and the latter is decomposed. Therefore, Al(acac)<sub>x</sub> complexes can exist. The DTG curve of modified ASA is similar, with the only difference that no conversion is observed at 423–433 K. Therefore, most of the Ni(acac)<sub>2</sub> on the surface of this material is in the coordinated state. Like  $\gamma$ -Al<sub>2</sub>O<sub>3</sub>, ASA allows the formation of Al(acac)<sub>x</sub> complexes, as is indicated by the weight losses at 570 and 620 K.

The IR spectra of the materials examined show absorption bands characteristic of vibrations of the acetylacetone ligand ( $1600\text{--}1200\text{ cm}^{-1}$ ) [5, 8], suggesting that the chelate structure of the complex is intact. In the spectra of modified  $\gamma\text{-Al}_2\text{O}_3$  and modified ASA, these bands are somewhat shifted relative to the same bands observed for SBA-15 and pure  $\text{Ni}(\text{acac})_2$ . Considering the thermoanalytical data, this shift can tentatively be attributed to the effect of the  $\text{Al}(\text{acac})_x$  complexes. In greater detail, this effect was studied in the gas-phase modification of supports.

#### Gas-Phase Modification

In this method, lengthening the treatment time and increasing the amount of complex did not change the Ni content of the resulting SBA-15,  $\gamma\text{-Al}_2\text{O}_3$ , and ASA, which was 0.52, 1.3, and 0.7 Ni atoms per squared nanometer, respectively, much higher than in liquid-phase modification (Fig. 4). This is explained by the fact that the reactivity of the complex increases with increasing temperature [7].

As in the case of liquid-phase modification, the chelate structure of the complex does not undergo any significant changes. This is indicated by the presence of IR absorption bands characteristic of the acetylacetone ligand. The peaks of these bands in the spectra of  $\gamma\text{-Al}_2\text{O}_3$  and ASA are shifted relative to the same peaks observed for SBA-15 and pure  $\text{Ni}(\text{acac})_2$  (Table 2). This shift is greater for the gas-phase modification than for the liquid-phase modification owing to a larger amount of surface acetylacetones in the former case. This allows a more detailed analysis of the IR spectra. As noted above, the most likely cause of the observed shift is the existence of  $\text{Al}(\text{acac})_x$  complexes. To verify this inference, we subtracted, from the IR spectrum of  $\text{Ni}(\text{acac})_2$ -modified  $\gamma\text{-Al}_2\text{O}_3$ , the spectrum of the same support treated with acetylacetone. The band positions in the difference spectrum appeared to coincide closely with the band positions in the spectrum of  $\text{Ni}(\text{acac})_2$  chemisorbed on the SBA-15 surface (Table 2). There-

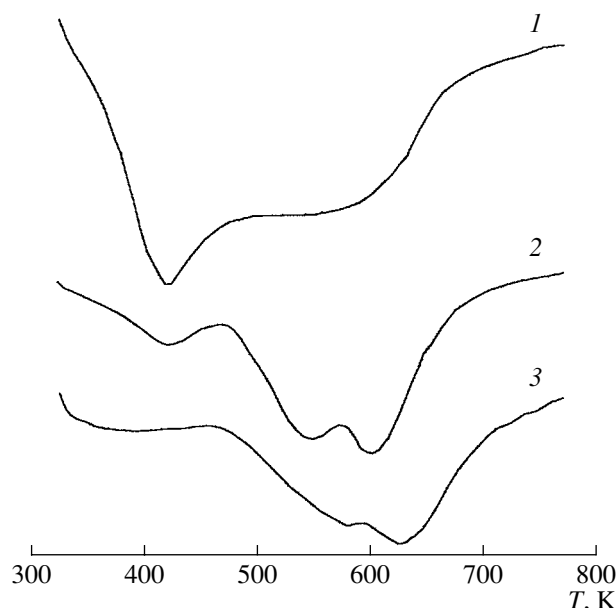
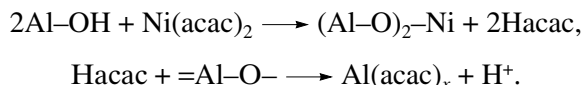


Fig. 5. DTG curves for the supports modified with  $\text{Ni}(\text{acac})_2$ : (1)  $\gamma\text{-Al}_2\text{O}_3$ , (2) SBA-15, and (3) ASA.

fore, a considerable proportion of the acetylacetone ligands remain to be coordinated to the nickel atom. Hence, the observed shift of the absorption bands is due to other surface compounds, specifically,  $\text{Al}(\text{acac})_x$ . These complexes result from the reaction between acetylacetone (Hacac), which is a product of the replacement of acetylacetone ligands, and  $\text{Al}^{3+}$  coordinatively unsaturated sites [5, 7, 8]. The formation of the aluminum complexes can be described by the following simplified scheme:



The proton formed reacts with oxygen on the support surface, resulting in a transformation of the hydroxyl group [5, 8].

Table 2. Absorption bands ( $\text{cm}^{-1}$ ) in the IR spectra of nickel acetylacetone in modified supports

$\text{Ni}(\text{acac})_2$	$\text{Ni}(\text{acac})_2/\text{SiO}_2$	$\text{Ni}(\text{acac})_2/\text{Al}_2\text{O}_3$	$\text{Ni}(\text{acac})_2/\text{ASA}$	$\text{Ni}(\text{acac})_2/\text{Al}_2\text{O}_3\text{-H}(\text{acac})/\text{Al}_2\text{O}_3$
1596	1589			1590
		1577	1575	
		1533	1534	1535
1520	1522			1522
1456	1450–1460	1457	1460	1458
1402	1398	1400	1402	1400
1360	1360–1370	1341	1341	1361
		1295		
1260	1260–1270	1267	1210	1260

**Table 3.** Hydrogen TPR and H<sub>2</sub> adsorption data for the catalysts

Support	Liquid-phase modification				Gas-phase modification			
	Ni content, Ni atoms/nm <sup>2</sup>	reduction onset temperature, K	peak temperature, K	H <sub>2</sub> /Ni	Ni content, Ni atoms/nm <sup>2</sup>	reduction onset temperature, K	peak temperature, K	H <sub>2</sub> /Ni
SBA-15	0.23	500	550	0.12	0.52	505	540	0.16
γ-Al <sub>2</sub> O <sub>3</sub>	0.71	520	572	0.16	1.30	518	560	0.22
ASA	0.14	535	590	0.20	0.70	520	580	0.25

The thermal analysis of the Al-containing materials has substantiated the above interpretation. As in the case of liquid-phase modification, the DTG curves of γ-Al<sub>2</sub>O<sub>3</sub> and ASA modified in the gas phase clearly indicate weight losses at 548 and 598–600 K, suggesting the existence and transformation of Al(acac)<sub>x</sub> complexes. As a consequence, the surface acetylacetone compounds decompose at a higher temperature in the Al-containing materials than in silica. The weight loss peak at 423–433 K, which is due to the conversion of hydrogen-bonded Ni(acac)<sub>2</sub>, is observed for none of the samples prepared in the gas phase. Therefore, by contrast with liquid-phase modification, the chemisorption of the complex from the gas phase occurs mainly through the replacement of acetylacetone ligands and the formation of a covalent bond between the metal atom and surface oxygen.

#### Characterization of the Oxide Phase in the Catalysts

As is specified above, the supported catalysts were prepared by calcining, in flowing air at 723 K, supports modified in toluene or in the gas phase. The IR spectra of these catalysts show no absorption bands due to acetylacetone complexes, indicating that the latter are completely decomposed. The degree of dispersion of the resulting oxide phase and, indirectly, the oxide–support interaction strength were determined by hydrogen TPR coupled with H<sub>2</sub> adsorption. In the TPR curves of all catalysts, the main hydrogen adsorption peak occurs at 570–590 K, close to the NiO reduction temperature [24]. Note that, for both modification techniques, the H<sub>2</sub> adsorption peak temperature depends on the nature of the support surface. This temperature is higher for the ASA-based catalysts than for the other materials (Table 3). This finding may be an indication of either a higher strength of the NiO–surface bonding or a lower degree of dispersion of NiO [25]. However, the H<sub>2</sub>/Ni ratio, which is a measure of the degree of dispersion [6, 13, 26], is the largest in the ASA-based specimens (Table 3). Therefore, it is the strong bonding between the NiO particles and the support surface that is the main cause of the increase in the reduction temperature. As is demonstrated above, Ni(acac)<sub>2</sub> chemisorption on ASA is mainly due to the interaction between this complex and the protons of  $\equiv$ Si–OH–Al= bridges. The complex chemisorbed in this way is localized, and this favors the strong fixation of the NiO par-

ticles resulting from the thermal decomposition of the complex. This interpretation is corroborated by the low degree of dispersion of nickel oxide in the catalysts based on SBA-15 and γ-Al<sub>2</sub>O<sub>3</sub>. Note that the gas-phase modification favors the dispersion of the oxide phase (Table 3). In the gas-phase modification, Ni(acac)<sub>2</sub> is mainly chemisorbed through ligand replacement. As a result, the metal atoms are covalently bonded to surface oxygen. For this reason, the NiO particles resulting from the thermal decomposition of the chemisorbed complex are unlikely to agglomerate. Therefore, the degree of dispersion of the oxide phase in the catalysts prepared by gas-phase modification depends strongly on the strength of the bonding between Ni(acac)<sub>2</sub> and the active sites of the support surface.

The formation of aluminum acetylacetones is a less significant factor. This inference follows from a comparison between the results obtained for the catalysts supported on SBA-15 and the Al-containing materials (Table 3). Apparently, the Ni(acac)<sub>2</sub> molecules react mainly with acid or base groups, while acetylacetone, which is a product of this interaction, reacts with coordinatively unsaturated sites formed by Al<sup>3+</sup> cations.

Thus, we have accomplished a nonhydrothermal synthesis of catalyst supports, namely, mesostructured silica of the SBA-15 type, which crystallizes in a hexagonal system (space group *P6mm*), and an ASA with Si<sup>4+</sup>/Al<sup>3+</sup> = 6.0. These materials are dominated by mesopores and have a rather large specific surface area. The ASA contains tetracoordinated, octacoordinated, and pentacoordinated aluminum ions and has proton-donor acid sites.

The above results indicate that nickel acetylacetone chemisorption on the oxide supports examined depends crucially on the nature of the surface active sites. The liquid-phase modification of the supports containing weakly acidic or weakly basic hydroxyl groups can be carried out only in low-polarity solvents. In the ASA, the dominant Ni(acac)<sub>2</sub> chemisorption sites are the acid hydroxyls of  $\equiv$ Si–OH–Al= bridges. The covalent bonds resulting from the replacement of the acetylacetone ligands with protons favor the fixation of the adsorbed complex on the surface. The coordinatively unsaturated sites formed by Al<sup>3+</sup> ions play an insignificant role in the chemisorption of the complex on the Al-containing materials. The degree of dispersion of the oxide phase in the catalysts depends strongly

on the strength of the interaction between the modifier molecules and the active sites of the support. The resulting aluminum acetylacetones have no significant effect on this parameter. The supported NiO particles are finer in the catalysts obtained by gas-phase modification than in their counterparts prepared in the liquid phase.

#### ACKNOWLEDGMENTS

M.V. Sychev acknowledges a guest grant from the Science Foundation of the Netherlands (NWO).

#### REFERENCES

1. Topsoe, H., Clausen, B.S., and Massoth, F.E., *Hydrotreating Catalysis*, Berlin: Springer, 1996.
2. Blanco, J., Avila, P., Suarez, S., et al., *Chem. Eng. J.*, 2004, vol. 97, no. 1, p. 1.
3. El-Shobaky, G.A., *Surf. Technol.*, 1978, vol. 7, no. 5, p. 375.
4. Zaman, J., *Fuel Process. Technol.*, 1999, vol. 58, nos. 2–3, p. 61.
5. Baltes, M., van der Voort, P., Weckhuysen, B.M., et al., *Phys. Chem. Chem. Phys.*, 2000, vol. 2, no. 11, p. 2673.
6. Puurunen, R.L., Zeelie, T.A., and Krause, A.O.I., *Catal. Lett.*, 2002, vol. 83, nos. 1–2, p. 27.
7. Baltes, M., van der Voort, P., Cillart, O., and Vansant, E.F., *J. Porous Mater.*, 1998, vol. 5, nos. 3–4, p. 317.
8. Van Veen, J.A.R., Jonkers, G., and Hesselink, W.H., *J. Chem. Soc., Faraday Trans. 1*, 1989, vol. 85, no. 2, p. 389.
9. Yamada, T. and Zhou, H-S., Hiroishi, D., et al., *Adv. Mater.*, 2003, vol. 15, no. 6, p. 511.
10. Barrett, E.P., Joyner, L.G., and Halenda, P.P., *J. Am. Chem. Soc.*, 1951, vol. 73, p. 373.
11. Gricus, Kofke, T.J., Gorte, R.J., and Farneth, W.E., *J. Catal.*, 1988, vol. 114, p. 34.
12. Juskelis, M.V., Slanga, J.P., Roberie, T.G., and Peters, A.W., *J. Catal.*, 1992, vol. 138, p. 391.
13. Ruels, R.C. and Bartholomew, C.H., *J. Catal.*, 1984, vol. 85, p. 63.
14. Zhao, D., Sun, J., Li, Q., and Stucky, G.D., *Chem. Mater.*, 2000, vol. 12, no. 2, p. 275.
15. Zhang, L.-X., Shi, J.-L., Yu, J., et al., *Adv. Mater.*, 2002, vol. 14, no. 20, p. 1510.
16. Rouquerol, F., Rouquerol, J., and Sing, K., *Adsorption by Powder and Porous Solids: Principles, Methodology and Applications*, San Diego: Academic, 1999.
17. Farmer, V.C., *The Infrared Spectra of Minerals*, London: Mineral Society, 1974, p. 331.
18. Shen, J., Tu, M., Hu, C., and Chen, Yi., *Langmuir*, 1998, vol. 14, no. 10, p. 2756.
19. Yan, Z., Ma, D., Zhuang, J., et al., *J. Mol. Catal. A*, 2003, vol. 194, nos. 1–2, p. 153.
20. Frydman, L. and Harwood, J.S., *J. Am. Chem. Soc.*, 1995, vol. 117, no. 19, p. 5367.
21. White, M.G., *Catal. Today*, 1993, vol. 18, p. 73.
22. Benito, I., del Riego, A., Martinez, M., Blanco, C., et al., *Appl. Catal., A*, 1999, vol. 180, nos. 1–2, p. 175.
23. Van Der Voort, P., White, M.G., and Vansant, E.F., *Langmuir*, 1998, vol. 14, no. 1, p. 106.
24. Suzuki, M., Tsutsumi, K., Takahashi, H., and Saito, Y., *Appl. Spectrosc.*, 1989, vol. 9, no. 2, p. 98.
25. Hu, Y., Dong, L., Shen, M., Liu, D., et al., *Appl. Catal., B*, 2001, vol. 31, no. 1, p. 61.
26. Anderson, J.A., Daza, L., Fierro, J.L.G., and Rodrigo, T., *J. Chem. Soc., Faraday Trans.*, 1993, vol. 89, no. 19, p. 3651.